

# Evaluation of the Crystallization Pressure of Sulfate Saline Soil Solution by Direct Observation of Crystallization Behavior

Shiyu Wu, Daoyong Wu,\* and Youfen Huang

Cite This: *ACS Omega* 2021, 6, 17680–17689

Read Online

ACCESS |



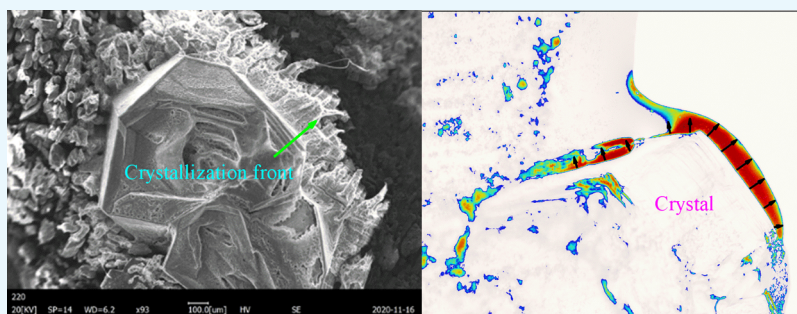
Metrics &amp; More



Article Recommendations



Supporting Information



**ABSTRACT:** We observed the growth of salt crystals in sulfate saline soil solution during evaporation at constant relative humidity and temperature and studied the formation mechanism of soil deformation induced by salt crystallization. The growth of salt crystals is recorded by images using a CCD camera under an optical microscope, and the solution supersaturation and crystallization pressure are calculated taking advantage of digital image processing. The growth of sodium sulfate multilayer crystals is observed conforming to the Kossel model. Moreover, it is estimated that the maximum growth rate in the longitudinal direction is almost ten times that in the lateral direction in large pore contribution to the nucleation barrier during crystal formation. The crystals act on the liquid film pushing away soil particles, achieving the “self-cleaning” effect finally. The liquid film shows elastic deformation property in a short time during crystal growth, demonstrating that crystallization pressure is exerted by the liquid film. During mirabilite crystal growth, the crystallization pressure values fluctuate within 0–12.57 MPa because the supersaturation of the film is consumed, destroying pores in sulfate saline soil and eventually expressed by salt expansion.

## 1. INTRODUCTION

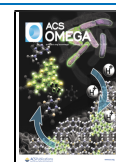
Crystallization of salt in pores and adhesion on the surface are some of the focal issues in numerous applications. The deterioration of porous materials (such as stone and brick) is caused by weathering<sup>1</sup> and is responsible for road surface cracking. In the field of building (cultural heritage), different salts are naturally existent in the stone or mortar,<sup>2</sup> or salts are from rain and underground water. As relative humidity (RH) decreases and evaporation rate increases, salt crystals precipitate inside (subflorescence) and on the surface (efflorescence) of materials, resulting in white residues of various shapes in old and new constructions.<sup>2,3</sup> Numerous ancient cultural heritages, such as the Mogao Grottoes in China<sup>4</sup> and the Angkor temples in Cambodia,<sup>5</sup> are often observed to be partially destroyed by salt attack under natural environmental conditions.<sup>6</sup> In particular to sodium sulfate, which is called the most deleterious salts on earth, its disservice is mainly due to its various hydrates with different solubility.<sup>7</sup> Under normal atmospheric conditions, two stable sodium sulfate phases can be observed: the decahydrate (mirabilite,  $\text{Na}_2\text{SO}_4 \cdot 10\text{H}_2\text{O}$ ) and anhydrous phase (thenardite,  $\text{Na}_2\text{SO}_4$ ).<sup>8–10</sup> A metastable sodium sulfate phase ( $\text{Na}_2\text{SO}_4 \cdot$

$7\text{H}_2\text{O}$ ) has been also observed during the cooling and drying experiment,<sup>11,12</sup> and another metastable phase III of  $\text{Na}_2\text{SO}_4$  is discovered in evaporation experiments at low RH.<sup>13</sup> Some previous studies<sup>14,15</sup> attribute the destructive effect to sodium sulfate hydration, which leads to an increase in volume (about 314%) as thenardite converts to its hydrate phase (mirabilite). However, many studies<sup>9,13,16</sup> have demonstrated that this transition occurs through the dissolution of anhydrous sodium sulfate and the recrystallization of mirabilite crystals. Compared with mirabilite, the dissolution of thenardite is more likely to result in supersaturated solution.<sup>17</sup> It is widely recognized that supersaturation is the driving force for crystal growth. The greater the driving force, the faster the crystal nucleation and growth rate.<sup>18</sup> Columnar habit crystals are mainly produced in the lower supersaturation solution, but

Received: April 28, 2021

Accepted: June 21, 2021

Published: July 1, 2021



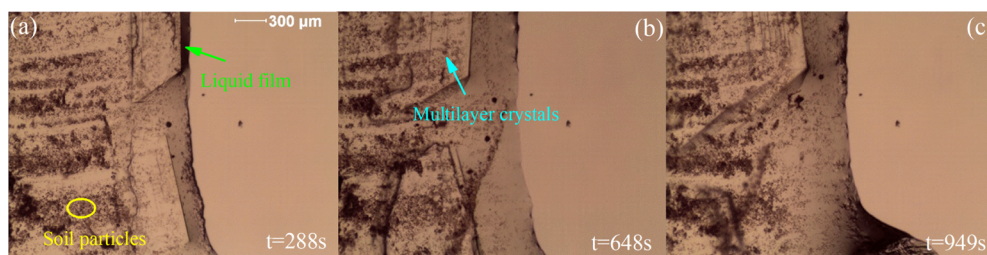


**Figure 1.** Nucleation and growth of crystals at the edge of soil solution ( $m_i = 10\%$ ). The time sequence of multilayer crystal growth (a)  $t = 288$  s, (b)  $t = 648$  s, and (c)  $t = 949$  s.

block habit crystals take the main advantage with supersaturation increasing.<sup>19,20</sup> When microcrystal salt (thenardite) dissolves in solution, they in part act as seeds to take shape into plentiful hydrate crystals and then form grape-like structures that expand rapidly.<sup>21</sup> The surface free energy enhances the solubility of sodium sulfate crystals, so that a tiny crystal is in equilibrium with a higher concentration of salt than a macroscopic crystal, which means that the solute will be inclined to diffuse toward large pores because crystals are prone to crystallize in large pores.<sup>18,22</sup> Hence, tiny crystals will cause the sodium sulfate hydrated phase to grow rapidly in the form of clusters. A stress is generated by the rapidly expanding clusters of mirabilite, exceeding the tensile strength of most porous materials.<sup>21</sup> What is more is that the chemical potential required for crystallization in the large-pore material is relatively small than that in small pores.<sup>23</sup> Micropores less than  $0.05 \mu\text{m}$  ( $0.1 \mu\text{m}$ ) have a significant impact on salt crystal damage, and the synergistic effect of these micropores with smaller ones generates greater crystallization pressure, inducing severe damage to stone.<sup>23,24</sup> Besides, the development of damage depends on additional factors, including the types of salt, RH and temperature, and the interface energy between the pore wall and the crystal.<sup>25</sup>

Sulfate saline soil is widely distributed in the northwest of China, and with the rapid development of western exploitation and infrastructure construction, the conservancy systems of roads and water are increasingly being constructed in saline soil.<sup>26</sup> The fundamental cause of salt expansion is the presence of sodium sulfate crystals. Therefore, many studies<sup>27–29</sup> have mainly focused on the salt expansion rate and deformation mechanism macroscopically in sulfate saline soil. However, under microscopic conditions, there is poor discussion on the growth of sodium sulfate crystals and how the crystals push soil particles away in the saline soil solution, although many scholars<sup>3,9,18,23</sup> have studied the crystal failure of sodium sulfate from the aspects of crystal morphology, supersaturation, and porous media characteristics. However, these research results mostly rely on the crystallization data of pure sodium sulfate solution or the destruction of pore materials before and after the experiment. The effect of the solution supersaturation in pores on the crystalline phase transition and the destructive effect of the phase transition process on pore materials cannot be directly detected.

In this paper, we report the nucleation and growth of sodium sulfate crystals on a piece of glass during evaporation at constant RH and temperature in a confined room. The sodium sulfate crystallization process in soil solution with different soil mass fractions is observed directly. It is found that crystal growth is an accumulation process. The observed results demonstrate the existence of a liquid film with elastic deformation properties at a certain crystallization pressure to

achieve a “self-cleaning” effect. Then, we use crystallization theory to investigate the effect of crystallization behavior on saline soil particles and the interaction between salt crystallization and the liquid film at normal temperatures.

## 2. EXPERIMENTAL METHODS

The test soil is silt sampled from Dashuiqiao in Qinghai province, China. The collected disturbed soil samples were washed more than 10 times with deionized water (electrical resistivity  $\rho \sim 7.8 \mu\text{S}/\text{cm}$ ) to exclude crystallization interference from other salt ions, and the washed soil samples were prepared by drying at  $105 \text{ }^\circ\text{C}$  and then crushed and screened ( $<0.25 \text{ mm}$ ). After the screening, we adopt a clear glass pestle to triturate silty soil particles again and again, making the size of the particle uniform. We start out this experiment with aqueous solutions of known initial concentration  $c_i = 1 \text{ mol/L Na}_2\text{SO}_4$  (the purity  $\geq 99.0\%$  produced by Tianjin Zhiyuan Chemical Reagent Co. Ltd). Different mass fractions ( $m_i = 10, 20, \text{ and } 50\%$ ) of desalt silty soil are added to a beaker containing  $50 \text{ mL}$  of  $1 \text{ mol/L}$  sodium sulfate solution.

The soil mass fraction is defined as  $m_i = \frac{m_s}{m_w} \times 100\%$ , where  $m_s$  and  $m_w$  are the mass of soil and water, respectively. After a fair oscillation, we use a dropper to absorb a certain amount of sulfate saline soil solution and then spread it quickly and evenly on a glass sheet and then place it on the optical microscope stage for crystallization behavior observation. The properties of glass sheets in the experiments are the same, ruling out the influence of the surface on crystal growth. The crystallization behavior is studied under isothermal conditions ( $T = 19 \pm 1 \text{ }^\circ\text{C}$ ) and a constant RH of  $70 \pm 2\%$  in two cases: (1) observing the nucleation and growth of crystals at the edge of soil solution and (2) studying the interaction between crystals and soil particles inside the soil solution. The constant RH and temperature in a confined room can minimize the impact of RH and temperature on the crystalline phase of sodium sulfate solution. The whole process of crystallization during the evaporation of the soil solution is recorded directly under an optical microscope with ten times magnification. The optical microscope has a CCD camera coupled with automated camera software to obtain images of the crystal growth and thin liquid film.<sup>30</sup>

## 3. RESULTS AND DISCUSSION

### 3.1. Crystallization Behavior of Sulfate Saline Soil.

The saturated solution concentration ( $C_{\text{sat}}$ ) of sodium sulfate is  $1.37 \text{ mol/L}$  at a temperature of  $19 \pm 1 \text{ }^\circ\text{C}$ , while the initial solution concentration is  $1 \text{ mol/L}$  in our experiment. When a few drops of unsaturated sulfate saline soil solution are deposited on the glass surface after oscillation uniformly, the edge of the soil solution begins to evaporate and reach the

saturation concentration within a few minutes. Then, the monolayer  $\text{Na}_2\text{SO}_4$  crystals begin to precipitate and continue to grow. As the liquid solution evaporates, one side of the crystal is surrounded by a black film of solution,<sup>22</sup> which is called supersaturation solution, as can be seen in Figure 1. Recent researchers highlight the effect of supersaturation as the driving force for the growth of crystals and the generation of stress.<sup>31</sup> In the previous pre-experiment, we found that the solution color where the crystals grew was varied under an optical microscope (Nikon SmartvS50D). Hence, we take advantage of this difference to obtain the concentrations of the unsaturation and supersaturation solution by digital image processing technology, and the relationship between the gray value and the solution concentration is determined (Figure 2)

$$\text{gray} = A + B \cdot c \quad (1)$$

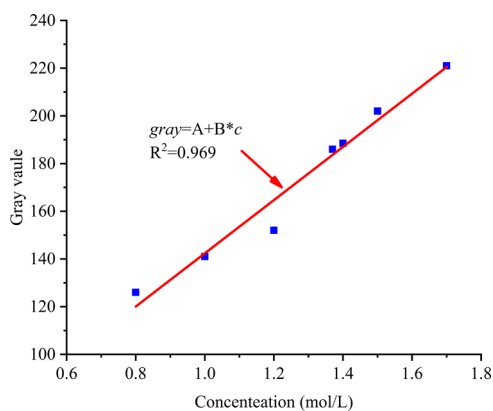


**Figure 2.** Relationship between the gray value and the solution concentration.

Thus, the supersaturation ratio  $S$  can be roughly estimated by

$$S = c/c_{\text{sat}} = (\text{gray} - A)/(B \cdot c_{\text{sat}}) \quad (2)$$

where  $A$  and  $B$  are the fitting parameters. It should be noted that the gray value is significantly affected by many factors including the observation environments (temperature, RH, and type of glass sheet) and the parameters of the optical microscope (intensity of the light source, definition of the eyepiece, etc.). The experimental conditions are strictly controlled in our observations, and the fitting parameters are  $A = 30.80$  and  $B = 111.58$ .

The calculated supersaturation ratios at the edge of the soil solution ( $m_1 = 10\%$ ) are shown in Figure 3. It is revealed that supersaturation also plays an important role in the process of multilayer crystal growth. A new layer of crystals will grow between the latest and bottom crystal layer (Movie S1), which is surrounded by supersaturation solution. After the initial crystallization of the crystal in sulfate saline soil solution, with the diffusion of the solute and the effect of evaporation, the solution concentration will reach the minimum supersaturation, and the crystal cell will crystallize on the original crystalline layer.

During the growth of multilayer crystals, the volume increase of  $\text{Na}_2\text{SO}_4$  crystals is observed. The characteristics of nucleation and growth of crystals at the edge of the soil solution probably imply that no damage is caused at the onset of crystal precipitation in large pores despite high supersaturation.<sup>32</sup> This is because crystals cannot fill the large pores of saline soil at the beginning. With the evaporation of the liquid solution, nuclei generated from a higher supersaturation solution compared with the growth of crystals are observed. Most crystals have more than one nucleation sites on the original crystals, and then, a new layer of crystals is generated.

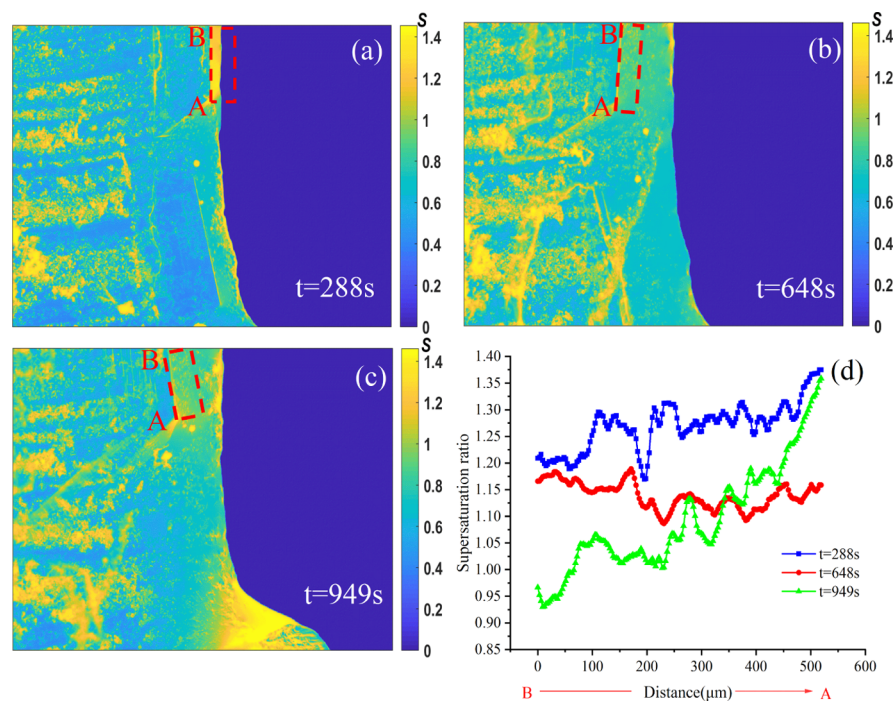


**Figure 3.** Calculated supersaturation ratios at the edge of soil solution ( $m_1 = 10\%$ ). (a)  $t = 288$  s, (b)  $t = 648$  s, and (c)  $t = 949$  s; (d) variation of the supersaturation ratio along the crystallization front AB. It is clear that the supersaturation ratio declines with the growth of multilayer crystals, which increases gradually from the crystal corner point A.

These crystals' growth mechanism applies to the Kossel model, since crystal growth becomes a multiple-step process.<sup>33</sup> To quantify the growth rate, we measure the crystal width as a function of time from the second to sixth crystal layer (Figure 4). We find that the crystal growth rate depends very strongly

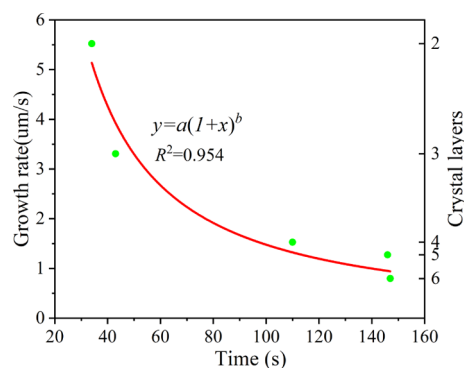


**Figure 4.** Growth rates of multilayer crystals in Figure 1.

on the degree of supersaturation (Figure 3). The crystallization rates for the second and sixth crystal layers are 5.52 and 0.80  $\mu\text{m/s}$ , respectively, while the corresponding average supersaturation ratios are 1.27 and 1.09, respectively. The result confirms that supersaturation is the driving force for crystal growth. The greater the driving force, the faster the crystal nucleation and growth rate.<sup>18</sup>

To study the interaction between crystals and soil particles, we focus on crystal growth behavior inside saline soil (Figure 5). We find that some crystals grow on the substrate, which can

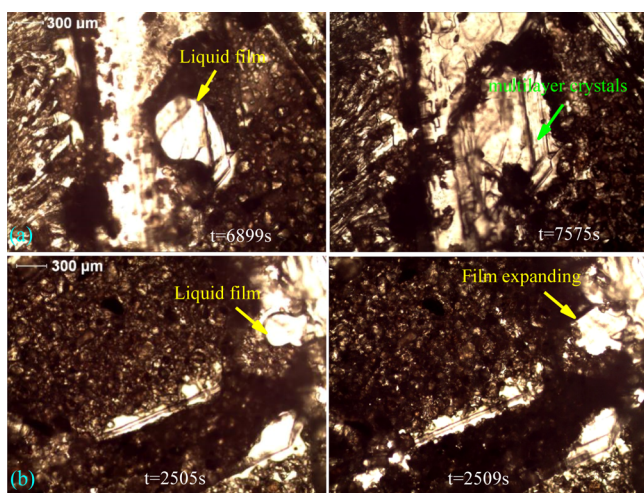


**Figure 5.** Crystal growth inside saline soil solution. Panels (a,b) illustrate the evolution process of multilayer crystals and liquid film in sulfate saline soil solution for  $m_i = 50$  and 20%, respectively.

cause various soil particles to move. It is surprising to note that some crystals' surface is very clean and others are covered with soil particles in the early stage of crystal growth. However, as water evaporates, the degree of supersaturation increases, and a new crystal layer starts to grow on top of the original crystal. With the continuous nucleation and growth of multilayer crystals, soil particles are pushed together. Consequently, the initial pore structure is destroyed by crystallization pressure, as seen in Figure 5a (Movie S2). The cumulative destruction process of pores in sulfate saline soil solution is contributed to

the “self-cleaning” effect of crystal generation, which needs secondary or more nucleation of thin layer crystals to provide different crystallization pressures. We also find that the crystallization pressure pushes the film to spread on the surface of crystals from 6899 to 7575 s, and the structure of soil particles around the film is damaged in the end; this could be an explanation for the damage caused by crystallization.

An important observation from the CCD camera images on the original crystal layer is that the thin film has the property of elastic deformation in a certain range of crystallization pressure, demonstrating the existence of a thin liquid film (Figure 5b). The thin film undergoes a process of expansion–shrink–expansion because of crystal growth when crystallization pressure is not enough to support the film dilation (Movie S3). After the formation of a new crystal layer, the salt solution evaporates on the surface, and a new film will be formed to drive soil grains away from crystals to get the “self-cleaning” effect.

Furthermore, remolded saline soil samples are prepared with 17% water content and a salt content of 4% in mass to study the morphology and location of crystal precipitation. The remolded saline soil samples are evaporated under the same environmental conditions along with the sulfate saline soil solution. After 12 h, we select topsoil samples and flocculent crystals to observe by scanning electron microscopy (SEM) and an optical microscope, respectively (Figure 6a,b). These

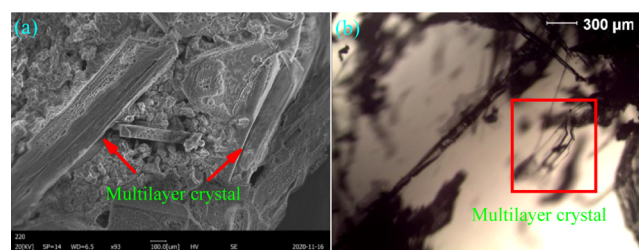


**Figure 6.** Existence of multilayer crystals in remolded sulfate saline soil with a mass salt content of 4%; panels (a,b) are, respectively, observed by SEM and optical microscopy.

images show the extraordinary similarity between the crystal structures in Figure 5a,b, namely, multilayer crystals, and the surface “self-cleaning” effect has also formed. Observation on sulfate saline soil shows that the mechanical mechanism of crystal growth in the edge of sulfate saline soil solution is similar with sulfate saline soil.

It is also interesting to note that the growth of crystals in a large pore does not destroy the pore structure (Figure 7a). This phenomenon may be attributed to the insufficient driving force supplied by supersaturation solution for crystal growth to fill the large pore; in other words, the crystallization pressure generated by crystals is not always destructive. Moreover, the crystal grows vertically at first and then horizontally, showing the directional difference of growth rate during crystal generation. The longitudinal and lateral growth rates of crystals A, B, C, and D are indicated in Figure 7b,c. As can be seen, the maximum growth rate in the longitudinal direction for crystal B is ten times that in the lateral direction. In this regard, the explanation given by the previous research is as follows: (1) whenever possible, a crystal will tend to grow in a direction where it does not encounter resistance and spread vertically<sup>14</sup> and (2) if the crystallization pressure exerted by an acicular crystal exceeds its yield strength, then, the crystal will

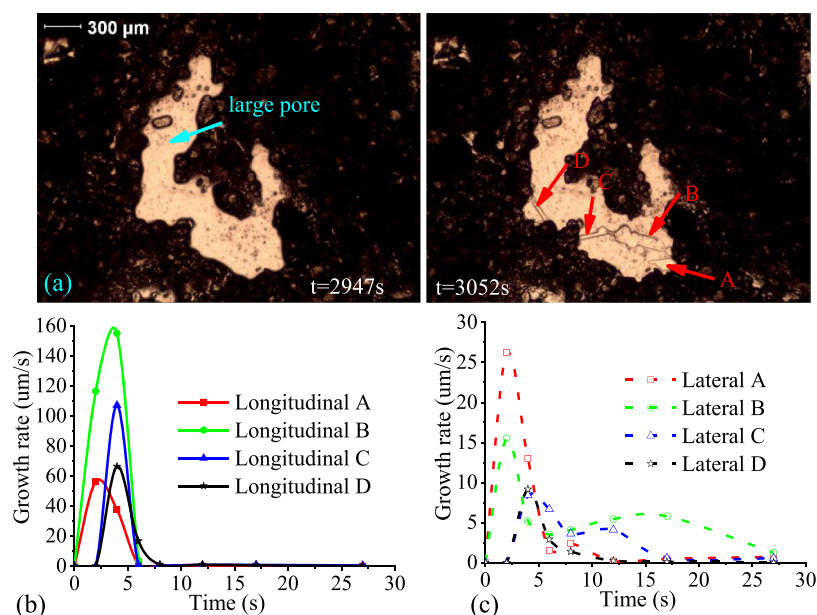


**Figure 7.** Growth of crystals is not always destructive in large pores. (a) Growth of crystals in a large pore; (b,c) Directional difference of the growth rate of crystals A, B, C, and D.

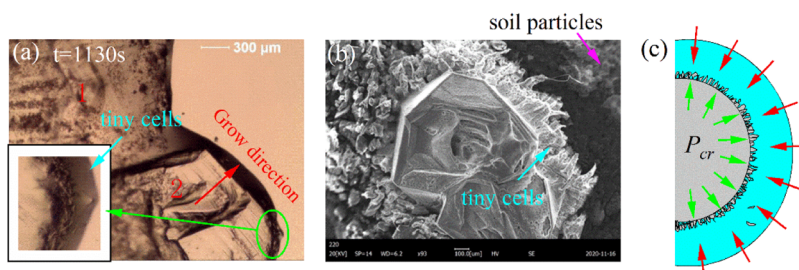


**Figure 8.** Tiny cells and crystallization pressure in the liquid film. (a) At the edge of soil solution ( $T = 20\ ^\circ\text{C}$ ,  $\text{RH} \sim 70\%$ ,  $m_i = 10\%$ ); (b) porosity zonation left by the liquid film is obvious between the tiny cells and soil particles inside saline soil with a mass salt content of 4%; and (c) illustration of crystallization pressure.

spread laterally.<sup>25</sup> From our observation, nuclei are formed from a relatively high supersaturation solution, which implies that the crystalline nuclear energy is very higher before breaking through the nucleation barrier.

**3.2. Crystallization Pressure Exerted by the Liquid Film.** Our observations raise a question of mechanical mechanisms for the “self-cleaning” effect of crystals and deformation of saline soil. To gain further insight into the crystal growth mechanism, we pay close attention to the variation in solution concentration, especially at the liquid–crystal interface. In the beginning, we observe many tiny cells in the front of the crystal (Figure 8a). These tiny cells are also found inside saline soil (Figure 8b). This means that tiny cells consist of nucleation sites when nucleating species already exist in the crystal front. The nucleation process reduced the energy of the liquid film, which implies that crystals grow at lower supersaturation.<sup>34</sup> From Figure 8a,b, we can conclude that the crystallization process from nuclei to crystals is the same whether in soil or solution. There is a crystallization pressure (illustrated by Figure 8c) between the crystals and the thin liquid film, causing the moving of soil particles and spreading of the liquid film front.

Several anhydrous and hydrate polymorphs of sodium sulfate may precipitate out of the saline soil. The phase diagram is useful to study the phase transformations in the

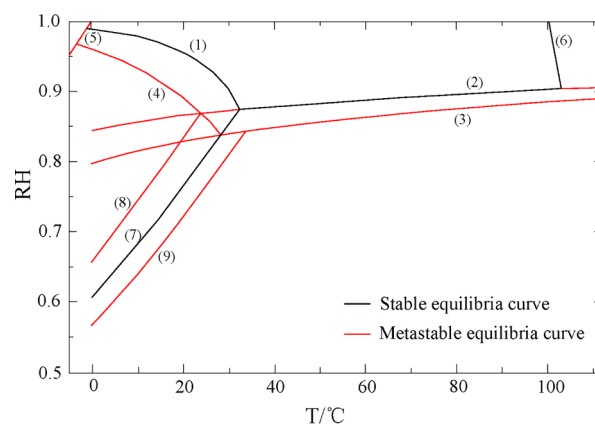


**Figure 9.**  $T/\text{RH}$  diagram of the  $\text{Na}_2\text{SO}_4\text{--H}_2\text{O}$  system.<sup>10</sup> The black and red curves, respectively, represent the stable and metastable equilibria. The solid-solution equilibrium (1–5) curves are, respectively, (1)  $\text{Na}_2\text{SO}_4\cdot 10\text{H}_2\text{O}$  (mirabilite), (2)  $\text{Na}_2\text{SO}_4(\text{V})$  (thenardite), (3)  $\text{Na}_2\text{SO}_4(\text{III})$ , (4)  $\text{Na}_2\text{SO}_4\cdot 7\text{H}_2\text{O}$  (metastable), and (5) freezing temperatures; (6) Solution–vapor equilibrium curve (boiling temperatures); the solid–solid equilibrium curves are (7)  $\text{Na}_2\text{SO}_4(\text{V})\text{--Na}_2\text{SO}_4\cdot 10\text{H}_2\text{O}$ , (8)  $\text{Na}_2\text{SO}_4(\text{V})\text{--Na}_2\text{SO}_4\cdot 7\text{H}_2\text{O}$ , and (9)  $\text{Na}_2\text{SO}_4(\text{III})\text{--Na}_2\text{SO}_4\cdot 10\text{H}_2\text{O}$ .

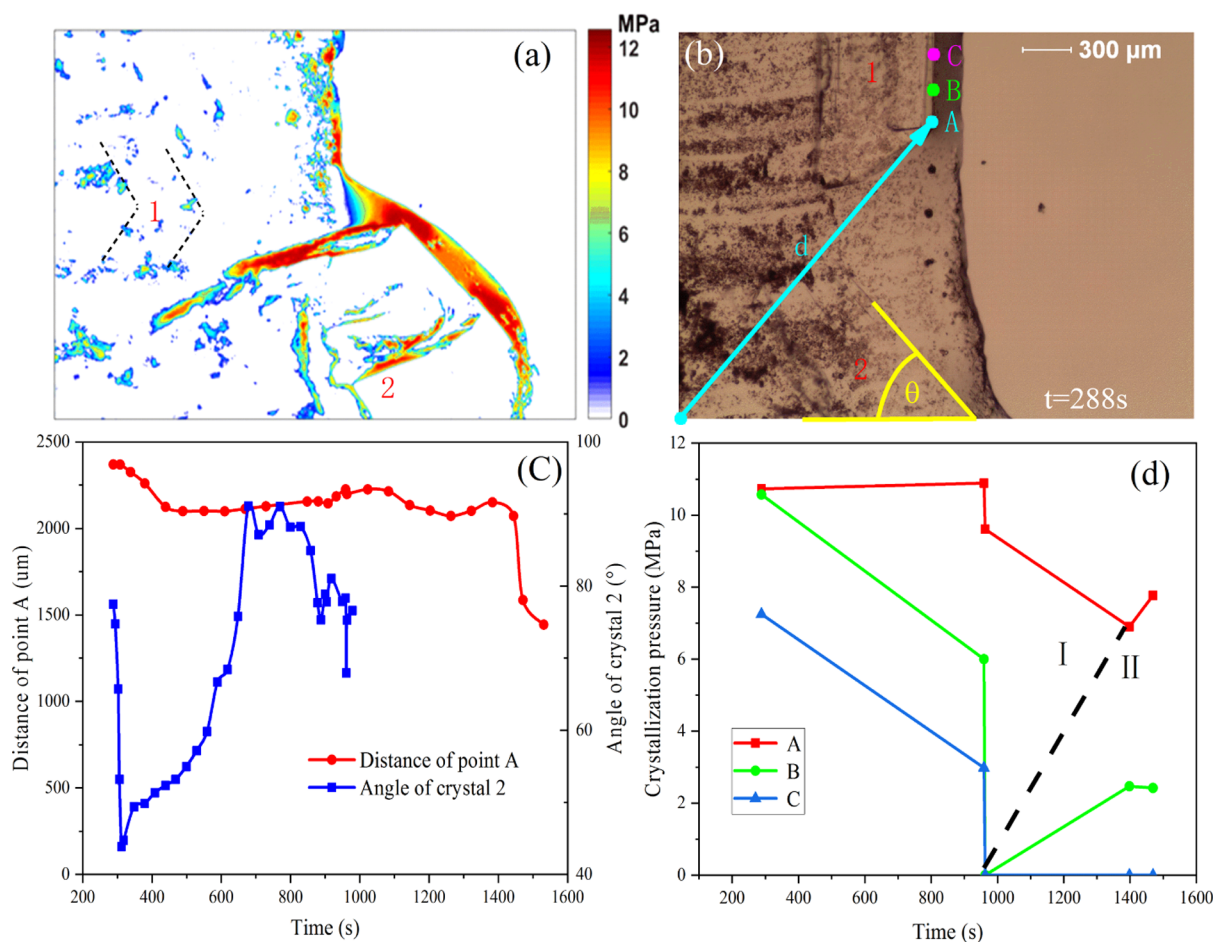


**Figure 10.** Crystallization pressure is exerted through the liquid film; (a) Distribution of crystallization pressure around crystals 1 and 2 in Figure 8a; (b) diagram of the distance of point A at the corner of crystal 1 and angle variation of crystal 2 and (c) distance variation and angular deflection of crystals 1 and 2; and (d) variation of crystallization pressure at points A, B, and C in panel (b).

$\text{Na}_2\text{SO}_4\text{-H}_2\text{O}$  system.<sup>16,17</sup> Thermodynamic data of aqueous  $\text{Na}_2\text{SO}_4$  and crystalline phases which are available by a careful review of the phase diagram of the  $\text{Na}_2\text{SO}_4\text{-H}_2\text{O}$  system including the metastable phase are provided in Figure 9.<sup>10</sup> At the room temperature of 20 °C, mirabilite is observed by X-ray diffraction and ESEM during evaporation of sodium sulfate solution droplets at relatively high RH (RH = 60%).<sup>3,9</sup> In contrast, only thenardite (phase V) and metastable  $\text{Na}_2\text{SO}_4$  phase III were found in droplet evaporation at low RH (RH < 50%).<sup>30</sup> Our experiments are carried out at constant RH and temperature ( $T = 19 \pm 1$  °C and RH = 70 ± 2%). The high concentrations required for the crystallization of phases III and V could not be achieved.<sup>10</sup> Therefore, we can ignore the influence of anhydrous phases (III and V) during crystallization pressure evaluation.

Studies by many scholars have shown that the force generated by crystal growth is large enough to destroy the porous materials.<sup>13,17,35–37</sup> For low supersaturation of sulfate saline soil solution, an equation for calculation of the crystallization pressure is expressed by the following form<sup>25,37</sup>

$$p_{\text{cr}} = p_c - p_l = \gamma_{\text{cl}} \kappa_{\text{cl}} = \frac{\nu RT}{V_m} \ln(s) \quad (3)$$

where  $\kappa_{\text{cl}}$  and  $\gamma_{\text{cl}}$  are, respectively, the curvature and free energy of the crystal/liquid interface;  $T$  is the absolute temperature and  $R$  is the gas constant;  $V_m$  is the molar volume of the

respective solid phase; and  $\nu$  is the total number of different ions per dissolved molecule.

With  $V_m = 219.8$   $\text{cm}^3/\text{mol}$  and  $\nu = 3$  for  $\text{Na}_2\text{SO}_4 \cdot 10\text{H}_2\text{O}$ , the range of supersaturation  $S$  is from 1 to 1.46 (Figure 3). Here, we calculate the value of crystallization pressure distribution around crystals, as can be observed in Figure 10a. The crystallization pressure of the mirabilite crystal in contact with the solution is relatively high, pushing the thin film to spread outside. On the contrary, the crystals are moved in the opposite direction by the reacting force of crystallization pressure if the crystallization pressure is not enough to expand the film. The moving and rotation processes of crystals 1 and 2 in Figure 10b are shown in Figure 10c. The principal direction of crystal 2 decreases from 77.49 to 43.85°, which increases to 91.10° following a second decreasing tendency. Correspondingly, the distance between the original point and point A at the corner of crystal 1 decreases from 2369.58 to 1444.13  $\mu\text{m}$ . Displacement of these mirabilite crystals further validates our previous discussion that crystallization pressure is a key factor to influence the diffusion of the liquid film and moving of crystals, reflecting that the dynamical variation of crystallization pressure can cause serious damage to porous materials such as brick and concrete. The upper limit crystallization pressure of mirabilite is 13.9 MPa for  $\text{Na}_2\text{SO}_4 \cdot 10\text{H}_2\text{O}$  at 20 °C and RH > 40%,<sup>10</sup> which is 14.3 MPa at 25 °C.<sup>35</sup> As shown in Figure 10d, we calculate the variations of crystallization

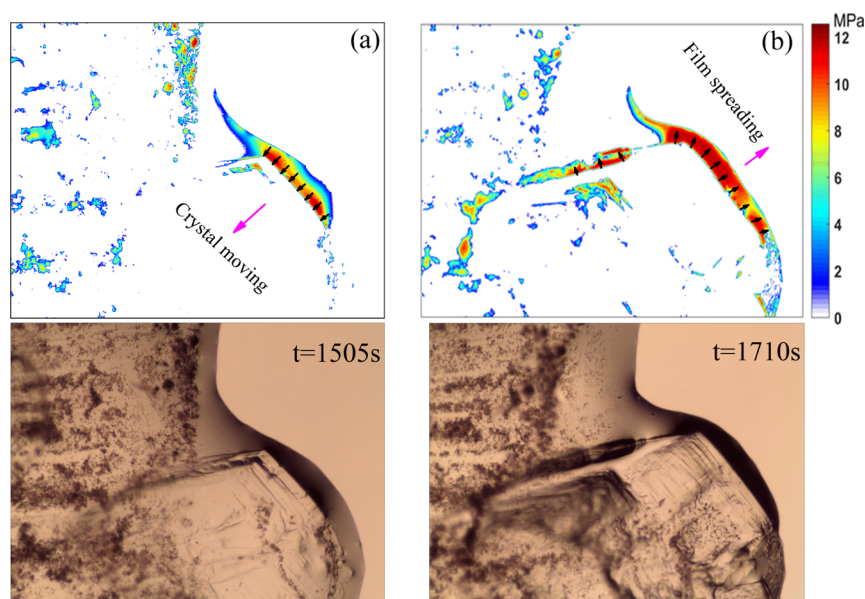


**Figure 11.** Crystallization pressure is exerted by the liquid film. (a) Moving of crystals due to the declined crystallization pressure in the process of growth ( $t = 1505$  s) and (b) spreading out of the liquid film during crystallization pressure accumulation ( $t = 1710$  s). Images are adopted by sulfate saline soil solution  $m_i = 10\%$ .

pressure at points A, B, and C in Figure 10b. The crystallization pressure  $P_{cr} \approx 0\text{--}12.57$  MPa is generated by the  $\text{Na}_2\text{SO}_4 \cdot 10\text{H}_2\text{O}$  crystals at room temperature. The calculated crystallization pressure of mirabilite is located in the upper limit obtained by previous studies. It should be noted that the calculated crystallization pressure may slightly be less than the upper limit because the soil particles will accelerate the crystal nucleation and consume supersaturation in our experiments. The crystallization pressure decreases simultaneously in stage I due to the growth of crystals consuming the supersaturation of solution, which increases after the stagnation period II (Figure 10d). The variation characteristics of crystallization pressure imply that more severe damage could be caused by the growth of the multilayer crystals.

We also find that crystallization pressure between crystals and the thin liquid film plays an important role in the process of film spreading (Figure 11). The crystallization pressure acts on the liquid film to push the solution diffusion outward, thus making the edge of the solution become meniscus (convex surface). The direction of crystal growth is always consistent with the outward expansion direction of the film, and the boundary of the sulfate saline soil solution eventually forms an “S” curve with the substrate (Figure 11a). The larger perimeter and the fastest evaporation are caused by the formation of the film, meaning that the crystal growth rate also becomes very high.<sup>30</sup> As a consequence, the abovementioned tiny crystal cells generated at the liquid–crystal interface decrease the interfacial tension during crystallization and evaporation,<sup>28</sup> leading to the rapid diffusion of the partial solution in contact with a crystal. Subsequently, the crystal begins to crystallize again when the film continues spreading. The more surprising correlation is that the supersaturation of the liquid film declines rapidly during the growth of the previously generated tiny cells and crystals, and the crystallization pressure generated by the crystal growth is not enough to push the film outward. Conversely, the crystal moves in the opposite direction (Movie S4). The results demonstrate that the

crystallization pressure is a critical factor to influence the diffusion of the liquid film and moving of crystals.

**3.3. Discussion.** From eq 3, the development of crystallization pressure is significantly affected by the supersaturation in the liquid film and pore size in porous materials. The crystallization pressure is roughly proportional to the supersaturation at a low supersaturation degree. As can be seen from Figures 4 and 10, the variations of crystallization pressure and growth rate for multilayer crystal formation share the same tendency with time. A power function-type empirical equation is adopted to represent the growth rate without considering the influence of crystal size<sup>38</sup>

$$G = k \cdot S^n \quad (4)$$

where  $G$  is the crystal growth rate and  $k$  and  $n$  are the crystallization rate parameters.

Thus, we can roughly get the relationship between crystallization pressure and crystal growth rate from eqs 3 and 4

$$P_{cr} = \frac{\nu RT}{n \cdot V_m} \ln\left(\frac{G}{k}\right) \quad (5)$$

Equation 5 implies that the greater the crystal growth rate, the greater the crystallization pressure. This phenomenon is confirmed by Figures 4 and 10, indicating that the rapid generation of crystals contributes to soil destruction. It shows that the result from the present model is in good agreement with experimental results obtained by Espinosa et al. (2008).<sup>18</sup>

Momentous differences in the degree of damage under the various RH conditions were discovered after the crystallization of sodium sulfate. As the RH decreases, rapid evaporation will promote higher supersaturation, ensuing larger crystallization pressure and causing severe damage because mirabilite and thenardite tend to form subflorescence in porous materials.<sup>3,17</sup> Besides, under low RH (40%) and low temperature (20 °C) conditions, the crystallization of anhydrous sodium sulfate is the main cause of damage to porous materials. This is because the solubility of thenardite is greater than that of mirabilite,

forming supersaturation solution easily and generating high crystallization pressure.<sup>9</sup> An increase in humidity will cause thenardite hydration in pores, and the volume change of sodium sulfate is more than 300% during hydration, causing expansion of saline soil.<sup>39</sup> When RH is very low, such as 20%, hydration does not usually occur; however, the direct precipitation of thenardite is observed in the droplets, and the crystallization pressure of mirabilite is smaller than that of thenardite for equal supersaturation, leading to pore destruction in the saline soil.<sup>39,40</sup>

It is noted that the solubility of sulfate is very sensitive to changes in temperature and humidity.<sup>17</sup> Sodium sulfate suffers a decrease in solubility at temperatures above (slow decrease) and below (rapid decrease) 32.4 °C.<sup>41</sup> As the temperature rises and the solubility increases, salt expansion will be decreased because numerous salt crystals dissolve. On the contrary, once the temperature drops, a large amount of salt will crystallize and generate high crystallization pressure in soil pores, resulting in severe salt expansion and inflicting damage and expansion of the soil surface structure.

Some researchers<sup>8,12</sup> have found that sodium sulfate heptahydrate is generated during temperature drops to 10 °C by nuclear magnetic resonance and in situ X-ray diffraction. As the temperature continues to drop, they find that heptahydrate is more easily converted to mirabilite at temperatures around or below 0 °C. In general, the crystallization pressure generated by sodium sulfate heptahydrate did not cause damage; however, mirabilite exerts a high crystallization pressure on the pore wall, leading to the destruction of the saline soil.<sup>11,37</sup>

In addition, the pore size distribution is crucial for us to understand the crystallization pressure. The existence of micropores and macropores can drastically change the pressure for crystallization in the pore size regions.<sup>42</sup> Many studies<sup>24,43</sup> have demonstrated that the crystallization pressure generated by the crystal growth in the small pores is greater than in the large pores, meaning that micropores have a significant impact on salt crystal damage. In the small pores, the needle-shaped sodium sulfate crystals probably tend to increase their destructive force due to the crystallization pressure being concentrated on a small surface area.<sup>41</sup> Under equilibrium conditions, greater stresses are expected when crystals grow either in small pores or try to grow into small pores from larger pores that are completely filled with crystals.<sup>15</sup> However, crystals preferentially crystallize in large pores because the chemical potential required to crystallize in large-pore materials is small.<sup>23</sup> Therefore, less destruction is observed during the growth of crystals from large pores (Figure 7a), demonstrating that small crystallization pressure exists in large pores.

It is well known that various porous materials (especially saline soil) have low tensile strength. Crystallization pressure exerted on the pore wall acts as tensile stress, strongly affecting the stability of these porous materials. The estimated crystallization pressure (0–12.57 MPa) for mirabilite is much larger than the tensile strength of numerous porous materials, causing serious damage to the microporous structures (Figure 5). Moreover, the variation of temperature and RH probably may cause the repeated emergence of the “self-cleaning” effect of crystals because of the accumulation of high supersaturation, and the corresponding crystallization pressure will push the soil particles away from their original place, expressing salt expansion eventually.

The temperature and RH are difficult to control in the field. Fortunately, from the abovementioned discussion, blocking up the migration of moisture and increasing the pore size scale are feasible ideas to prevent salt crystallization destruction. Consequently, several measures, such as raising the foundation height, digging a salt ditch, and replacing fillers with rock block, are useful when engineering constructions build in saline soil regions.

#### 4. CONCLUSIONS

In summary, we reported on the crystallization behavior in sulfate saline soil solution under constant evaporation rate in a confined space. By capturing the images of  $\text{Na}_2\text{SO}_4 \cdot 10\text{H}_2\text{O}$  crystal growth, multilayer crystals are observed to conform to the Kossel model, that is, the crystal growth process is the result of extrapolation of layers of crystal planes. This phenomenon is discovered both in soil solution and saline soil. During the accumulation of supersaturation, we find that crystals act on the liquid film, pushing away the soil particles and achieving the “self-cleaning” effect finally. The liquid film shows an expanding–shrinking–expanding phenomenon in a short time during crystal growth, which implies that the liquid film has elastic deformation property under a certain crystallization pressure. Moreover, the directional difference of growth rate during crystal generation is determined by the nucleation barrier. The maximum growth rate in the longitudinal direction is almost ten times that in the lateral direction. To gain further insight into the crystal growth and destruction mechanism of sodium sulfate, the liquid–crystal interface is studied in detail. Many tiny cells are observed in the front of crystallization, which act on the film to generate crystallization pressure. During the growth of each layer of crystal, the evaluated pressure value varies from 0 to 12.57 MPa because the supersaturation of solution is consumed in this process, resulting in the destruction of pores in sulfate saline soil and eventually expressed by salt expansion. However, the observation revealed that the crystallization pressure is not always destructive in large pores. Results from this research help us to understand the growth mechanisms of crystals and the complex variation of crystallization pressure, providing a theoretical guidance to solve the problem of salt heaving and ensuring the safe operation of foundation engineering and related buildings in sulfate saline soil regions.

#### ■ ASSOCIATED CONTENT

##### Supporting Information

The Supporting Information is available free of charge at <https://pubs.acs.org/doi/10.1021/acsomega.1c02251>.

New layer of crystal growth between the latest and bottom crystal layer (AVI)

Process of film destruction (AVI)

Existence of a liquid film with elastic deformation property (AVI)

Crystal moving backward due to crystallization pressure acting on the liquid film (AVI)

#### ■ AUTHOR INFORMATION

##### Corresponding Author

Daoyong Wu – College of Resources and Environmental Engineering, Key Laboratory of Karst Georesources and Environment, Ministry of Education, Guizhou University, Guiyang 50025, China; [orcid.org/0000-0003-0719-](https://orcid.org/0000-0003-0719-)



8147; Phone: +86 851 83627126; Email: dywu@gzu.edu.cn; Fax: +86 851 8115556

## Authors

**Shiyu Wu** – College of Resources and Environmental Engineering, Key Laboratory of Karst Georesources and Environment, Ministry of Education, Guizhou University, Guiyang 50025, China

**Youfen Huang** – College of Resources and Environmental Engineering, Key Laboratory of Karst Georesources and Environment, Ministry of Education, Guizhou University, Guiyang 50025, China

Complete contact information is available at:  
<https://pubs.acs.org/10.1021/acsomega.1c02251>

## Author Contributions

The manuscript was written through contributions of all authors. All authors have given approval to the final version of the manuscript.

## Notes

The authors declare no competing financial interest.

## ACKNOWLEDGMENTS

This research was supported by the National Natural Science Foundation of China (grant nos. 41761016 and 42002280) and the Science and Technology Program of Guizhou Province (grant nos. [2017]5788 and [2019]1056).

## REFERENCES

- (1) Saidov, T. A.; Leo, P.; Klaas, K. Crystallization Pressure of Sodium Sulfate Heptahydrate. *Cryst. Growth Des.* **2015**, *15*, 2087–2093.
- (2) Salim, H.; Paul, K.; Bonn, D.; Shahidzadeh, N. Self-Lifting NaCl Crystals. *J. Phys. Chem. Lett.* **2020**, *11*, 7388.
- (3) Rodriguez-Navarro, C.; Doehne, E. Salt weathering: influence of evaporation rate, supersaturation and crystallization pattern. *Earth Surf. Processes Landforms* **1999**, *24*, 191–209.
- (4) Li, F.; Wang, X.; Guo, Q.; Zhang, B.; Pei, Q.; Yang, S. Moisture adsorption mechanism of earthen plaster containing soluble salts in the Mogao Grottoes of China. *Stud. Conserv.* **2019**, *64*, 159–173.
- (5) Siedel, H.; Pfefferkorn, S.; von Plehwe-Leisen, E.; Leisen, H. Sandstone weathering in tropical climate: Results of low-destructive investigations at the temple of Angkor Wat, Cambodia. *Eng. Geol.* **2010**, *115*, 182–192.
- (6) Shahidzadeh, N.; Desarnaud, J. Damage in porous media: role of the kinetics of salt (re)crystallization. *Eur. Phys. J.: Appl. Phys.* **2012**, *60*, 24205.
- (7) Granneman, S. J. C.; Shahidzadeh, N.; Lubelli, B.; van Hees, R. P. J. Effect of borax on the wetting properties and Crystallization behavior of sodium sulfate. *CrystEngComm* **2017**, *19*, 1106–1114.
- (8) Derluyn, H.; Saidov, T. A.; Espinosa-Marzal de, R. M.; Pel, L.; Scherer, G. W. Sodium sulfate heptahydrate I: The growth of single crystals. *J. Cryst. Growth* **2011**, *329*, 44–51.
- (9) Rodriguez-Navarro, C.; Doehne, E.; Sebastian, E. How does sodium sulfate crystallize? Implications for the decay and testing of building materials. *Cem. Concr. Res.* **2000**, *30*, 1527–1534.
- (10) Steiger, M.; Asmussen, S. Crystallization of sodium sulfate phases in porous materials: The phase diagram Na<sub>2</sub>SO<sub>4</sub>–H<sub>2</sub>O and the generation of stress. *Geochim. Cosmochim. Acta* **2008**, *72*, 4291–4306.
- (11) Espinosa Marzal, R. M.; Scherer, G. W. Crystallization of sodium sulfate salts in limestone. *Environ. Geol.* **2008**, *56*, 605–621.
- (12) Hamilton, A.; Hall, C.; Pel, L. Sodium sulfate heptahydrate: direct observation of crystallization in a porous material. *J. Phys. D: Appl. Phys.* **2008**, *41*, 212002.
- (13) Linnow, K.; Zeunert, A.; Steiger, M. Investigation of Sodium Sulfate Phase Transitions in a Porous Material Using Humidity- and Temperature-Controlled X-ray Diffraction. *Anal. Chem.* **2006**, *78*, 4683–4689.
- (14) Tsui, N.; Flatt, R. J.; Scherer, G. W. Crystallization damage by sodium sulfate. *J. Cult. Herit.* **2003**, *4*, 109–115.
- (15) Flatt, R. J.; Scherer, G. W. Hydration and Crystallization Pressure of Sodium Sulfate: a Critical Review. *Mater. Res. Soc. Symp. Proc.* **2002**, *712*, II.2.
- (16) Schiro, M.; Ruiz-Agudo, E.; Rodriguez-Navarro, C. Damage Mechanisms of Porous Materials due to In-Pore Salt Crystallization. *Phys. Rev. Lett.* **2012**, *109*, 265503.
- (17) Flatt, R. J. Salt damage in porous materials: how high supersaturations are generated. *J. Cryst. Growth* **2002**, *242*, 435–454.
- (18) Espinosa, R. M.; Franke, L.; Deckelmann, G. Phase changes of salts in porous materials: Crystallization, hydration and deliquescence. *Constr. Build. Mater.* **2008**, *22*, 1758–1773.
- (19) Borchert, C.; Sundmacher, K. Efficient formulation of crystal shape evolution equations. *Chem. Eng. Sci.* **2012**, *84*, 85–99.
- (20) Ulrich, J. Growth Rate Dispersion - A Review. *Cryst. Res. Technol.* **1989**, *24*, 249–257.
- (21) Shahidzadeh-Bonn, N.; Desarnaud, J.; Bertrand, F.; Chateau, X.; Bonn, D. Damage in porous media due to salt crystallization. *Phys. Rev. E: Stat., Nonlinear, Soft Matter Phys.* **2010**, *81*, 066110.
- (22) Scherer, G. W. Stress from crystallization of salt. *Cem. Concr. Res.* **2004**, *34*, 1613–1624.
- (23) Rossi-Manaresi, R.; Tucci, A. Pore structure and the disruptive or cementing effect of salt crystallization in various types of stone. *Stud. Conserv.* **1991**, *36*, 53–58.
- (24) Yu, S.; Oguchi, C. T. Role of pore size distribution in salt uptake, damage, and predicting salt susceptibility of eight types of Japanese building stones. *Eng. Geol.* **2010**, *115*, 226–236.
- (25) Scherer, G. W. Crystallization in pores. *Cem. Concr. Res.* **1999**, *29*, 1347–1358.
- (26) Wan, X.; Hu, Q.; Liao, M. Salt crystallization in cold sulfate saline soil. *Cold Reg. Sci. Technol.* **2017**, *137*, 36–47.
- (27) Zhang, S.; Zhang, J.; Gui, Y.; Chen, W.; Dai, Z. Deformation properties of coarse-grained sulfate saline soil under the freeze thaw-precipitation cycle. *Cold Reg. Sci. Technol.* **2020**, *177*, 103121.
- (28) Lai, Y.; Wu, D.; Zhang, M. Crystallization deformation of a saline soil during freezing and thawing processes. *Appl. Therm. Eng.* **2017**, *120*, 463–473.
- (29) Zhang, J.; Lai, Y.; Li, J.; Zhao, Y. Study on the influence of hydro-thermal-salt-mechanical interaction in saturated frozen sulfate saline soil based on crystallization kinetics. *Int. J. Heat Mass Transfer* **2020**, *146*, 118868.
- (30) Shahidzadeh-Bonn, N.; Rafai, S.; Bonn, D.; Wegdam, G. Salt Crystallization during Evaporation: Impact of Interfacial Properties. *Langmuir* **2008**, *24*, 8599–8605.
- (31) Steiger, M. Crystal growth in porous materials—II: Influence of crystal size on the crystallization pressure. *J. Cryst. Growth* **2005**, *282*, 470–481.
- (32) Desarnaud, J.; Derluyn, H.; Carmeliet, J.; Bonn, D.; Shahidzadeh, N. Hopper Growth of Salt Crystals. *J. Phys. Chem. Lett.* **2018**, *9*, 2961–2966.
- (33) Cuppen, H. M.; Meekes, H.; van Enkevort, W. J. P.; Vlieg, E. Kink incorporation and step propagation in a non-Kossel model. *Surf. Sci.* **2004**, *571*, 41–62.
- (34) Agrawal, S. G.; Paterson, A. H. J. Secondary Nucleation: Mechanisms and Models. *Chem. Eng. Commun.* **2015**, *202*, 698–706.
- (35) Steiger, M. Crystal growth in porous materials -I The crystallization pressure of large crystals. *J. Cryst. Growth* **2005**, *282*, 455–469.
- (36) Espinosa-Marzal, R. M.; Scherer, G. W. Advances in Understanding Damage by Salt Crystallization. *Acc. Chem. Res.* **2010**, *43*, 897–905.
- (37) Desarnaud, J.; Bonn, D.; Shahidzadeh, N. The pressure induced by salt crystallization in confinement. *Sci. Rep.* **2016**, *6*, 30856.
- (38) Tang, A.; Guangzhou, D. *Study on Crystal Growth Behaviour*; South China University of Technology, 2014.

- (39) Oguchi, C. T.; Yu, S. A review of theoretical salt weathering studies for stone heritage. *Prog. Earth Planet. Sci.* **2021**, *8*, 32.
- (40) Winkler, E. M.; Singer, P. C. Crystallization pressure of salt in stone and concrete. *Geol. Soc. Am. Bull.* **1972**, *83*, 3509–3514.
- (41) Cooke, R. U. Salt weathering in deserts. *Proc. Geol. Assoc.* **1981**, *92*, 1–16.
- (42) Meldrum, F. C.; O'Shaughnessy, C. Crystallization in Confinement. *Adv. Mater.* **2020**, *32*, 2001068.
- (43) Chatterji, S. Aspects of generation of destructive crystal growth pressure. *J. Cryst. Growth* **2005**, *277*, 566–577.